ELSEVIER

Contents lists available at ScienceDirect

## Soil & Environmental Health

journal homepage: www.sciencedirect.com/journal/soil-and-environmental-health



## Research Paper

## Effects of burn severity on organic nitrogen and carbon chemistry in high-elevation forest soils



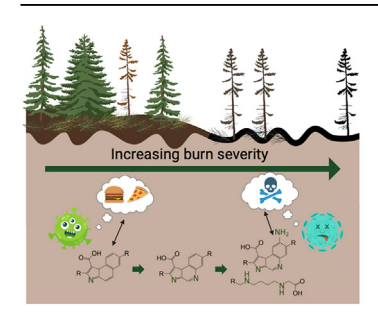
Holly K. Roth <sup>a</sup>, Amy M. McKenna <sup>b,c</sup>, Myrna J. Simpson <sup>d</sup>, Huan Chen <sup>b</sup>, Nivetha Srikanthan <sup>d</sup>, Timothy S. Fegel <sup>e</sup>, Amelia R. Nelson <sup>c</sup>, Charles C. Rhoades <sup>e</sup>, Michael J. Wilkins <sup>c</sup>, Thomas Borch <sup>a,c,\*</sup>

- <sup>a</sup> Department of Chemistry, Colorado State University, Fort Collins, CO, 80523, USA
- b National High Magnetic Field Laboratory, Ion Cyclotron Resonance Facility, Florida State University, FL, 32310, USA
- <sup>c</sup> Department of Soil and Crop Sciences, Colorado State University, Fort Collins, CO, 80523, USA
- d Environmental NMR Centre and Department of Physical & Environmental Sciences, University of Toronto Scarborough, Toronto, Ontario, Canada
- e Rocky Mountain Research Station, U.S. Forest Service, Fort Collins, CO, 80526, USA

#### HIGHLIGHTS

- Higher burn severities result in the formation of *N*-dense molecules.
- The soil microbiome is largely unable to process *N*-dense molecules.
- Soil toxicity increases as burn severity increases.

#### GRAPHICAL ABSTRACT



#### ARTICLE INFO

Handling Editor: Lena Q. Ma Technical Editor: Randy A Dahlgren

Keywords:
Heterocyclic N
Soil organic matter
Wildfire severity gradients
FT-ICR MS
Microtox toxicity
NMR spectroscopy

#### ABSTRACT

Fire frequency and severity have increased in recent decades in the western United States, with direct implications for the quantity and composition of soil organic matter (SOM). While the effects of wildfire on soil carbon (C) and inorganic nitrogen (N) have been well studied, little is known about its impacts on soil organic N. Since organic N is the most abundant form of soil N in conifer forests and dominant source of plant N facilitated by symbiotic mycorrhizae and mineralization, better understanding of post-fire organic N chemistry will help address a critical gap in our understanding of fire effects on SOM. Here, we characterized changes to organic N chemistry across fire severity gradients resulting from two wildfires that burned lodgepole pine (*Pinus contorta*) forest along the Colorado/Wyoming border, USA. One representative gradient was selected for high-resolution analysis based on results from bulk data (total C and N, and pH). Mineral soils were collected from two depths in low, moderate, and high severity burned areas and adjacent, unburned locations one year following the Ryan and Badger Creek fires. Nuclear magnetic resonance spectroscopy and 21 tesla ultrahigh-resolution Fourier transform ion cyclotron resonance mass spectrometry analysis showed that N content and aromaticity of water-extractable SOM (0–5 cm depth) increased with burn severity, while minimal changes to 5–10 cm depth were observed. Heterocyclic N species are generally higher in toxicity compared to their non-nitrogenated counterparts, which prompted soil toxicity measurements. Complementary Microtox® analysis revealed a positive relationship between increased

#### https://doi.org/10.1016/j.seh.2023.100023

Received 7 February 2023; Received in revised form 14 June 2023; Accepted 14 June 2023 Available online 20 June 2023

2949-9194/© 2023 The Author(s). Published by Elsevier B.V. on behalf of Zhejiang University and Zhejiang University Press Co., Ltd. This is an open access article under the CC BY license (http://creativecommons.org/licenses/by/4.0/).

<sup>\*</sup> Corresponding author. Department of Soil and Crop Sciences, Colorado State University, Fort Collins, CO, 80523, USA. *E-mail address:* Thomas.borch@colostate.edu (T. Borch).

fire severity and increased soil toxicity to *Alivibrio fischeri* (microbial test species). These findings add to our molecular-level understanding of organic C and N responses to wildfire severity, with likely implications for nutrient cycling, forest recovery and water quality following severe wildfire.

#### 1. Introduction

Wildfire activity in the western United States has increased in recent decades in terms of the size of area burned (Williams and Abatzoglou, 2016) and the frequency and severity of large fires (Abatzoglou et al., 2017), and is projected to continue to increase (Westerling, 2016). Observed warming conditions have led to greater frequency of wildfire in high-elevation forests in recent years (Alizadeh et al., 2021); therefore, it is critical that we understand the impacts of changing fire regimes on ecosystem dynamics, biodiversity, and productivity at higher elevations. The expected increase in burn severity (i.e., degree of consumption of organic soil layers and vegetation) (Parsons et al., 2010) may have implications for carbon cycling, potentially shifting forests from C sinks to C sources. The post-fire soil organic matter (SOM) composition provides a baseline for a forest's recovery; thus, molecular-level analysis of SOM from different burn severities will help improve our understanding of ecosystem response following wildfire.

Wildfires influence biogeochemical and hydrological cycles through the combustion of biomass, which alters SOM properties (e.g., C:N:P stoichiometry, pH, major functional groups), forms hydrophobic layers, and increases C and N in postfire runoff (González-Pérez et al., 2004). The combination of heat from wildfires and changes in SOM properties have consequences for plant and microbiome diversity which may persist for years after the fire. Previous studies indicate that burn severity differentially impacts the upper 5 cm of mineral soil (Hartford and Frandsen, 1992) and local soil microbiomes by destabilizing soil aggregates and affecting microbial biomass and composition and associated enzyme activity (Pulido-Chavez et al., 2021). SOM transformations that occur during heating can result in increased chemical heterogeneity, forming a substrate that is generally more resistant to microbial decomposition (Singh et al., 2012). SOM and soil microbiota are important for re-establishment of native plant species; therefore, fire-induced transformations may influence post-fire plant succession, plant species composition, and ecosystem processes (Turner, 2010). Short-term (1-5 years post-fire) impacts often include significant SOM losses from surface organic horizons (Nave et al., 2011). Additional short-term responses include increased erosion (Moody et al., 2013), increased inorganic N (Wan et al., 2001), and decreased bacterial and fungal community richness in burned plots compared to unburned (Caiafa et al., 2023; Nelson et al., 2022; Pulido-Chavez et al., 2021). Negative impacts to soil microbes may persist for over a decade: ectomycorrhizal and saprobic richness were lower than in unburned soils 11 years after fire in a ponderosa pine (Pinus ponderosa) forest (Pulido-Chavez et al., 2021), total soil N depletion persisted at least 14 years following fire with subsequent reduction of tree and shrub colonization in a Scots pine (P. sylvestris) forest (Dzwonko et al., 2015), and dissolved total nitrogen (DTN) export was ~10× higher in burned compared to unburned catchments 14 years after the Hayman Fire in Colorado (Rhoades et al., 2018). Recovery of microbial communities requires bioavailable C and N, therefore, understanding the role of burn severity on SOM C and N composition is important for developing effective post-fire management strategies.

Organic N is a dynamic component of soils, derived primarily from amino acids and peptides and easily mineralized into plant-available inorganic N (Zhong and Makeschin, 2003). Organic N comprises 62–83% of the total N in Norway spruce stands (Smolander et al., 2001), and dissolved organic N (DON) is a primary pathway for N loss in forest soils while acting as a N source for mycorrhizal plants in boreal forests (Andersson et al., 2000). Direct analysis of organic N can be accomplished by Fourier transform ion cyclotron resonance mass spectrometry

(FT-ICR MS), which provides molecular-level insight that can be used to calculate oxidation state, aromaticity, and biolability (D'Andrilli et al., 2015). Acidic N species in burned SOM detected by negative-ion electrospray ionization (-ESI) FT-ICR MS indicate that N incorporates into refractory, heterocyclic aromatic compounds that are more resistant to microbial degradation (Luo et al., 2019; Roth et al., 2022b). Bahureksa and coworkers reported that aromatic N heterocycles were formed in soil burned at higher temperatures in a laboratory microcosm (Bahureksa et al., 2022); however, these findings have not yet been verified across burn severities. Additionally, positive-ion mode ESI (+ESI) detected more than twice the number of *N*-species across a wider H/C and O/C range compared to -ESI in fire-affected soils (Roth et al., 2022a). Thus, in this study we focus on +ESI to selectively ionize SOM species through protonation reactions to catalogue molecular transformations that occur during soil heating and the potential implications for N cycling.

Nuclear magnetic resonance (NMR) spectroscopy can be paired with FT-ICR MS to quantify shifts in functionality, which is required to link SOM compositional changes to microbial degradation pathways to improve C and N cycling predictions in response to high severity fires (Schmidt et al., 2011). NMR has been used to demonstrate an increase in aromatic structures and decrease in alkylated organic molecules in severely burned pine forest soils (Knicker et al., 2008). NMR spectra showing decreased atomic H/C and O/C ratios across a burn severity gradient in soils from wildfire-affected forest and shrub ecosystems are the net result of greater dehydration, dealkylation, and decarboxylation reactions at higher wildfire severity (Merino et al., 2015). The abundance of N-heterocyclic compounds also increased with burn severity, but varied with fuel composition (e.g., grasses or coniferous litter) and heating conditions (Bahureksa et al., 2022; Merino et al., 2015; Roth et al., 2022a). However, rigorous analysis of the specific compounds formed at different burn severities remains limited, especially in field studies.

Wildfires have been reported to release toxic compounds (e.g., polycyclic aromatic hydrocarbons; PAHs, heavy metals, nitrogenated species), with associated short- and long-term implications for ecosystem recovery due to their environmental persistence and propensity to bioaccumulate. Importantly, N-heterocycles have been linked to increased toxicity in hydrothermal liquefication of biomass (Alimoradi et al., 2020) and have been shown to modulate the toxicity of co-occurring metals in soils (i.e., cadmium, boron) (Cervilla et al., 2009), although specific structures have yet to be reported. Ecotoxicants may prompt shifts in microbial populations that adversely affect ecosystem processes or may be transported downslope in leachate or eroding soil or downstream in surface runoff. Microtox® is a bioassay that uses bioluminescence inhibition of the bacterium Aliivibrio fischeri (A. fischeri) to evaluate chemical contamination in soils, waters, and biochars (Gavrić et al., 2022), and is commonly used as an indicator for metal, pesticide, or PAH contamination (Doherty, 2001). Limited studies exist on the eco-toxicological impacts of fire on water quality, despite evidence that post-fire runoff is toxic to organisms in multiple trophic groups (Campos et al., 2012). Therefore, the impact of burn severity on soil toxicity is relatively

Here, we characterize the relationship between fire severity and SOM composition along soil burn severity gradients and discuss the implications of *N*-heterocycle formation for toxicity to soil microbes. Soil was collected from two recently burned lodgepole pine dominated forests along the Colorado-Wyoming border (Fig. 1). We hypothesized that soil C and N chemical composition would track with burn severity with more microbially-recalcitrant organic matter and heterocyclic N compounds formed at higher burn severities. To evaluate this hypothesis, we

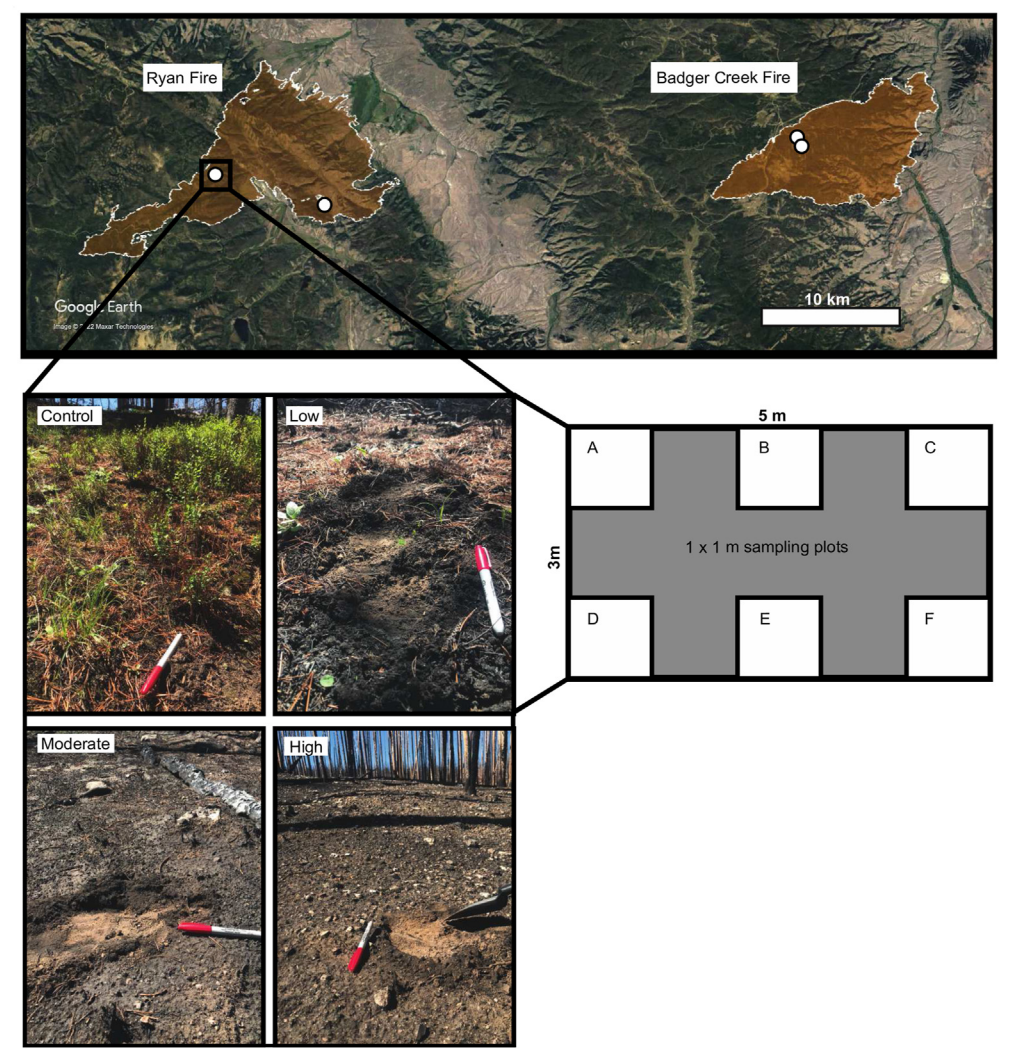


Fig. 1. Map indicating sampling sites and strategy in the 2018 Ryan and Badger Creek Fire burn scars. Top: Google Earth image of the Ryan Fire and Badger Creek Fire burn scars (latitude of samples ranged from 41.01162 to 41.04866; longitude ranged from -106.12196 to -106.63271). White dots indicate burn severity transect locations. Bottom left: photos of each burn severity class (Unburned/Control, Low, Moderate, High Severity). Bottom right: visual representation of the 3  $\times$  5 m sampling grid with subplots labeled A-F.

measured elemental chemistry across four distinct burn severity gradients at wildfires near the Colorado-Wyoming border and then performed a suite of high-resolution analyses which included NMR, 21 tesla FT-ICR MS and Microtox® on one representative burn severity gradient. We found that molecular-level C and N composition differed with burn severity. The chemical patterns we identified may have relevance to soil toxicity to microbes, though verification of its general importance requires exploration across wide temporal and ecosystem ranges.

#### 2. Methods

#### 2.1. Soil sampling and preparation

Soil samples were collected in mid-2019, one-year post-fire in lodgepole pine-dominated forests burned by the 2018 Badger Creek and Ryan fires in the Medicine Bow National Forest (elevation 2500–2750 m). The sampling period captures the conditions the first summer following fire and snowmelt, when the sites were first accessible. Soils in the sampling areas were loamy-skeletal Ustic Haplocryepts and fine-loamy Ustic Haplocryalfs.

Four independent burn severity gradients comprised of low, moderate, and high severity burns and an unburned control were selected based on remotely sensed comparison of pre- and post-fire greenness (Key and Benson, 2006). Severity was field-validated prior to sampling using standard soil burn severity indicators (Parsons et al., 2010). Low, moderate, and high severity sites had >85%, 20–85%, and <20% O-horizon

cover, respectively (Parsons et al., 2010). At each sampling site, a  $3\times 5$  m sampling grid with 6  $m^2$  subplots was laid out perpendicular to the dominant slope (Fig. 1). To limit differences in site aspect, slope gradient, and pre-fire vegetation within each of the burn severity gradients, we located individual burn severity classes within 50 m of one another.

A sterilized trowel was used to collect approximately 150 g of 0–5 cm and 5–10 cm soils by first sampling and collecting the 0–5 cm soil, then collecting the underlying 5–10 cm soil. Samples (n = 48) were placed on ice in the field and stored at 4  $^{\circ}$ C in the laboratory until processing. The unburned control and low severity samples had a thin O-horizon (~5 mm), and the moderate and high severity samples had a similar thickness of charred organic matter and ash. After air drying, samples were passed through a 2-mm mesh sieve to remove residual litter and other large debris. See Nelson et al. for additional details (Nelson et al., 2022).

#### 2.1.1. Elemental Measurements

Dissolved organic carbon (DOC) and dissolved total nitrogen (DTN) concentrations were determined from warm water extracts (1:2, soil:water) for the soil samples. Measurements were performed with a TOC-VCPN total organic C/N analyzer (Shimadzu Corporation, Columbia, MD, USA). A subset of samples from each depth (n = 16) were dried (48 h at 60  $^{\circ}$ C), ground to a fine powder, and analyzed for total C and N by dry combustion (LECO Corporation, St. Joseph, MI, USA). To determine the pH of the soils, a 1:2 ratio of soil (g) to deionized water (mL) was shaken for 1 h at 200 rpm before pH measurements were recorded. We used the DOC and DTN concentrations and pH (Table S1) to identify general

patterns and select a subset of representative samples ( $n=6;\,n=4$  for 0–5 cm and n=2 for 5–10 cm) for selected analyses.

#### 2.1.2. Soil extractions

We identified significant differences in DOC and DTN concentrations between the 0-5 cm unburned control and moderate and high severity water extracts, as well as a significant difference in pH between the control and all burned 0-5 cm soil water extracts (Table S1). We also noted significant differences in %C and %N between the unburned control and moderate and high 0-5 cm soils (Table S2). Based on these differences in soils between each burn severity class at the 0-5 cm depth, a single gradient consisting of one control and one each of the low, moderate, and high severity soils was selected for further analysis described below. Since there were no differences in the 5-10 cm soils or water extracts; two samples were selected for further analysis (control and moderate) as differences in soil chemistry were expected to be minimal. A total of six samples from the 48 collected were selected for further analyses, including acute toxicity, 21 T FT-ICR MS, and solid-state <sup>13</sup>C NMR: a high severity 0-5 cm soil, moderate severity 0-5 cm and 5-10 cm soils, a low severity 0-5 cm soil, and controls from the 0-5 cm and 5-10 cm soils (Table S3).

Dissolved organic matter (DOM) using water extracts of the 0-5 cm soils from this subset was also analyzed by solution-state <sup>1</sup>H NMR. For acute toxicity and FT-ICR MS, 50 g dry, sieved soil was weighed into a polystyrene weigh boat and transferred to a 250 mL Erlenmeyer flask. For solution-state <sup>1</sup>H NMR, we used the DOC concentrations to determine the amount of soil needed to extract 10 mg of DOC. For all samples, Millipore water was added to a final ratio of 1 g soil: 2 mL water in Erlenmeyer flasks (one flask for FT-ICR MS and acute toxicity, another for <sup>1</sup>H NMR), which were covered with parafilm and shaken (10 h, 170 rpm) in the dark. Water and soil slurries were quantitatively transferred to pre-rinsed 50-mL centrifuge tubes with an additional 150 mL Millipore water. The samples were then centrifuged at 7500 rpm (756×g) for 10 min, during which a vacuum filtration system was assembled using acid-washed, precombusted glassware. The 0.2 µm polyethersulfone (PES) filters were pre-rinsed with 100-150 mL Millipore water prior to sample introduction. A 50-mL aliquot from the FT-ICR MS samples was stored in centrifuge tubes; the remaining filtrate was stored in amber bottles at 4 °C until solid phase extractions. Solid soils were analyzed by solid-state <sup>13</sup>C NMR, and soil water extracts were analyzed by solution-state <sup>1</sup>H NMR, 21 T FT-ICR MS, and Microtox ®. Additional information on NMR instrumentation can be found in Supporting Information.

## 2.1.3. Acute toxicity of water-soluble species

Microtox® acute toxicity analysis was used to determine the toxicity of soil water extracts in the control and burned samples for *A. fischeri* bacteria. During sample preparation for FT-ICR MS, 50 mL of each sample was subsampled and stored in centrifuge tubes. From these samples, 1 mL was transferred to amber HPLC vials (3 mL for Control 5-10 cm only) for Microtox® analysis. Samples were carbon normalized to 9.29 ppm of C based on DOC values and stored at 4 °C until analysis. The percent decrease in bioluminescence of *A. fischeri* bacteria after a 15-min incubation period determines the toxicity of each sample based on the amount of light emitted by the bacteria (Adams et al., 2015). The Microtox® 81.9% screening test protocol was used on the Microtox® model 500 analyzer (Modern Water, New Castle, DE, USA) as previously described (Chen et al., 2022b).

## 2.2. FT-ICR MS analyses

## 2.2.1. Solid-phase extractions

Solid-phase extractions were performed on the six subsamples selected for compositional analysis prior to FT-ICR MS analysis according to Dittmar et al. (2008). Briefly, samples were brought to room temperature and acidified to pH 2 with trace-metal free hydrochloric acid (Sigma-Aldrich Chemical, St. Louis, MO, USA). PPL cartridges (Bond Elut

PPL (Priority Pollutant™), a styrene-divinylbenzene (SDVB) polymer modified with a proprietary nonpolar surface) were rinsed with 15 mL HPLC-grade methanol (Sigma-Aldrich Chemical) and 15 mL of pH 2 Millipore water. Polar species in the water samples were retained on the sorbent, rinsed with 15 mL of pH 2 water to remove salts, and allowed to dry overnight. Each sample was recovered from the cartridge by elution with 2 mL HPLC-grade methanol and transferred to 2-mL borosilicate vials prior to 21 T FT-ICR MS analysis.

#### 2.2.2. ESI source

All solvents were HPLC grade (Sigma-Aldrich Chemical) and SPE extracts were analyzed after further dilution in methanol (1:10, by volume) prior to analysis by negative and positive ion electrospray ionization. Sample solution was infused via a microelectrospray source (Emmett et al., 1998) (50  $\mu m$  i. d. fused silica emitter) at 500 nL/min by a syringe pump. Typical conditions for negative ion formation were: emitter voltage,  $-2.7\text{-}3.1\,kV;$  S-lens RF: (45%) and heated metal capillary temperature 350 °C. Positive-ion ESI spray conditions were opposite in polarity.

#### 2.2.3. 21 T FT-ICR MS

The six DOM extracts were analyzed with a custom-built hybrid linear ion trap FT-ICR mass spectrometer equipped with a 21 T superconducting solenoid magnet (Hendrickson et al., 2015; Smith et al., 2018) and automatic gain control (AGC ion target: 1E6) (Belov et al., 2003; Page et al., 2005). Peaks with signal magnitude greater than 6 times the baseline root-mean-square (rms) noise at m/z 500 were processed in absorption mode, exported to peak lists, and molecular formula assignments and data visualization were performed with PetroOrg© software (Corilo, 2014). Molecular formula assignments with an error >0.2 parts-per-million were discarded, and only chemical classes with a combined relative abundance of  $\geq$ 0.10% of the total were considered. All FT-ICR mass spectra files and assigned elemental compositions are publicly available via the Open Science Framework at https://osf.io/758ux/(DOI: DOI 10.17605/OSF.IO/758UX). Further details can be found in Supporting Information.

### 2.3. MAG annotation for N heterocycle degradation genes

To investigate whether the soil microbiome was expressing genes for degrading N heterocycles, we utilized the metagenome-assembled genome (MAG) and metatranscriptomic dataset presented in Nelson et al. (2022) (NCBI BioProject PRJNA682830). We analyzed a MAG dataset which was assembled from metagenomic sequencing done on 12 samples that consisted of a triplicate of high severity and low severity (3 from 0 to 5 cm and 3 from 5 to 10 cm for each treatment). We used HMMER (Eddy, 2011) against hidden Markov models (HMMs) curated from UniProt (Bateman et al., 2015) to search for the genes needed to constitute the multicomponent enzyme carbazole 1,9a-dioxygenase (CARDO) (Nojiri et al., 2005; Xu et al., 2006). CARDO is made up of four parts: two terminal oxygenases (carAa; PF11723), a ferredoxin (carAc; PF00355), and a ferredoxin reductase (carAd; PF00970, PF00111, PF00175). Following the identification of the genes, we used the metatranscriptomics mapping data presented in Nelson et al. (2022) to identify whether the genes were being expressed within the given MAG.

#### 3. Results and discussions

## 3.1. Burned soil organic matter is more complex than unburned

We performed solid-state  $^{13}$ C NMR spectroscopy on six mineral soil samples to visualize the differences in organic matter functionality across the burn severity gradient, with spectra reported in Fig. S1 and integration results in Table 1. We chose to analyze the  $^{13}$ C isotope due to the low abundance of  $^{15}$ N in natural samples. In the 0–5 cm soils, there was a decrease in alkyl C and *O*-alkyl C from the unburned control to the low

Table 1

Integration results for solid-state  $^{13}$ C NMR spectroscopy analysis of burn severity and soil depth (n = 1). Chemical shift, used to determined NMR regions, is reported in parts per million (ppm). This table lists the relative proportion of alkyl C, *O*-alkyl C, aromatic & phenolic C, and carboxylic + carbonyl C to the total signal of  $^{13}$ C across all regions. The alkyl/*O*-alkyl carbon ratio is determined by dividing the relative proportion of alkyl C by that of the *O*-alkyl C.

	Relative Proportion of SOM categories to the total <sup>13</sup> C NMR signal						
Sample	Alkyl C (0–50 ppm)	O-alkyl C (50–100 ppm)	Aromatic & phenolic C (110–165 ppm)	Carboxylic + Carbonyl C (165–210 ppm)	Alkyl/O- alkyl carbon ratio		
Control (0–5 cm)	40	35	20	5	1.14		
Low (0–5 cm)	25	11	59	5	2.27		
Moderate (0–5 cm)	37	17	39	7	2.18		
High (0–5 cm)	35	13	46	6	2.69		
Control (5–10 cm)	42	35	19	4	1.20		
Moderate (5–10 cm)	41	25	31	3	1.64		

severity soil, consistent with the results reported for *Pinus pinaster* duff, which indicated a dominance of alkyl C and *O*-alkyl C compounds in the unburned sample (Merino et al., 2018). Conversely, aromatic and phenolic C was approximately 3× higher in the low severity soil, indicative of incomplete combustion (Bodí et al., 2014). The alkyl/*O*-alkyl C ratio, used as an indicator of SOM decomposition (a higher ratio indicates a higher relative stage of decomposition) (Simpson et al., 2008), nearly doubled in the low severity soil compared to the control. From low to moderate severity, the relative proportion of alkyl C and *O*-alkyl C increased in the moderate severity 0–5 cm soil, then decreased slightly

from moderate to high. These shifts primarily resulted in decreases in the relative proportion of aromatic and phenolic C in the moderate and high severity samples; carboxylic + carbonyl C were slightly higher in the moderate and high severity 0–5 cm soils compared to the control. Importantly, the alkyl/O-alkyl C ratio remained approximately double that of the control in all burned samples, which indicates that fire drives SOM chemistry towards more complex forms that are less preferred microbial substrates in this burn severity gradient. This is also reflected in the aromatic C integration data (higher in burned soils), as aromatic C is generally considered to be less labile for microbial respiration than other C forms (Schmidt and Noack, 2000). However, a separate study on the same samples presented here found that microbial genes targeting aromatic compounds were present in the soils (Nelson et al., 2022), which indicates that aromatic substrates can be utilized as C sources in the burned soils.

#### 3.2. DOM displays burn severity-dependent trends in 0-5 cm soils

We collected FT-ICR mass spectra for six soil water extracts along the burn severity gradient - four from 0 to 5 cm soils (control, low, moderate, and high) and two from 5 to 10 cm soils (control and moderate). To increase compositional coverage, we ionized samples in ESI negative and positive modes (Roth et al., 2022a). There were an average of 11,320 assigned species in -ESI and 21,377 in +ESI, and a substantial increase in the number of nitrogenated species in the burned soils relative to the unburned control, consistent with previously reported increases of CHNO in fire-impacted water extracts of Jeffrey pine (P. jeffreyi) needles and woody trunks in -ESI (Chen et al., 2022a). We plotted all elemental compositions identified in the +ESI analysis of the water-soluble soil extracts in van Krevelen diagrams (H/C vs O/C) (Kim et al., 2003) to provide visualization of the data and highlight compositional differences between the samples in Fig. 2. Fire-impacted samples spanned a wide range of H/C ratios (0.2-1.9), with a larger relative abundance of highly saturated compounds in the low and high severity burn samples.

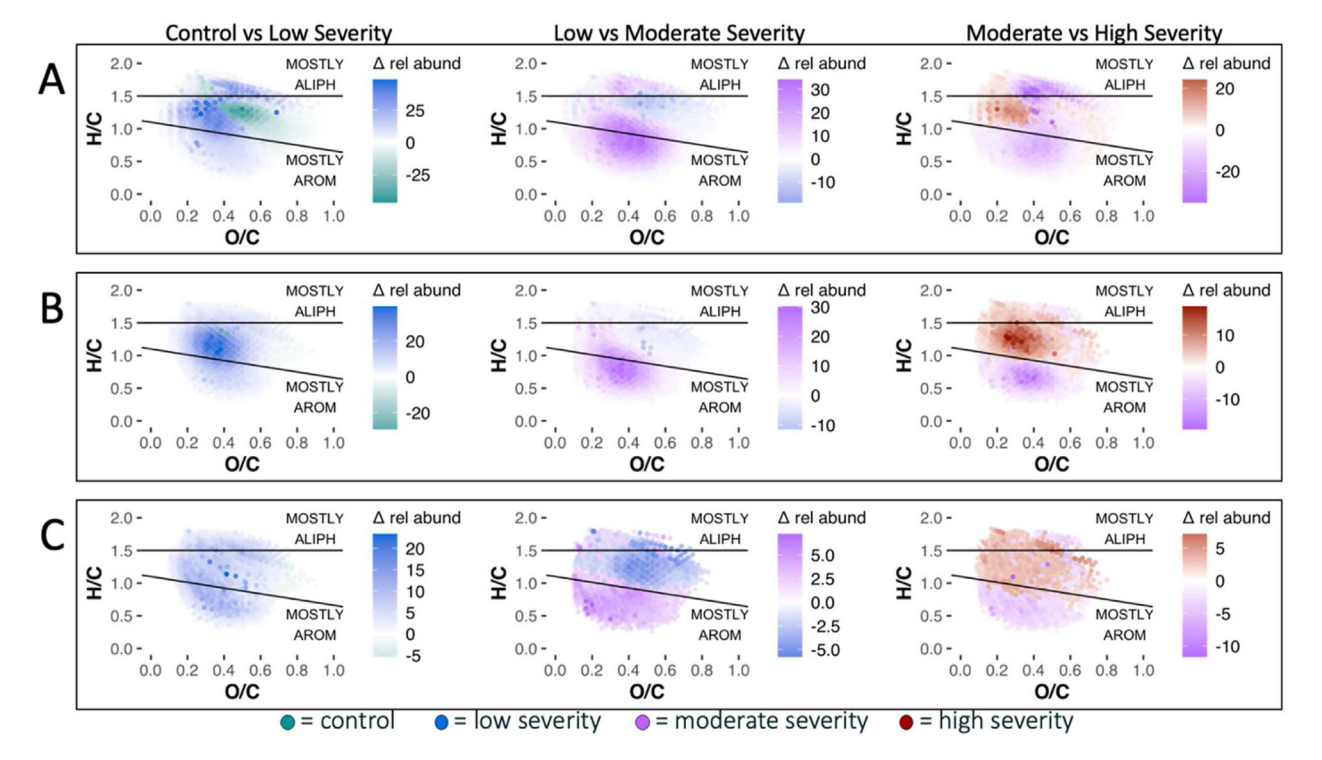


Fig. 2. Van Krevelen diagrams of the detected species of water-soluble soil extracts (0-5 cm) identified by + ESI FT-ICR MS. The top row (A) contains all formulas, the middle row (B) contains only CHNO molecular formulas, and the bottom row (C) contains only the unique CHNO species. Each panel compares two samples, indicated by color. Larger changes in relative abundance ( $\Delta$  rel abund) are indicated by more saturated colors. Formulae plotted below the line that intercepts at H/C 1.2 are generally more aromatic in structure, while those plotting above the line that intercepts at H/C 1.5 are more aliphatic.

Maximum O/C ratios decreased with burn severity, as did average O/C (Table S4), consistent with carbonization and aromatization processes and a decrease in the lability of soil species reported for *P. pinaster* soils (Merino et al., 2018). Within the *N*-containing species, we again observed an enrichment in highly saturated compounds in the low and high severity soils. O/C ratios in the nitrogenated species did not appear to be as dependent on burn severity as the total assignments, which demonstrates that the O/C ratio is likely not a primary driver for biotic or abiotic transformations of these species.

To further analyze the difference in DOM chemistry between burn severity classes, we also performed solution-state <sup>1</sup>H NMR spectroscopy on DOM isolated from 0 to 5 cm soils in the burn severity gradient (Table 2). Relative to the control, there was little to no change in the relative proportion of materials derived from linear terpenoids (MDLT). Carboxyl-rich alicyclic molecules (CRAM) were lower in the burned samples, consistent with lower average O and O/C and lower average molecular weight in the FT-ICR mass spectra. Conversely, the relative contribution of soluble carbohydrates and peptides was higher in the burned samples, with a maximum intensity in the low severity soil extract, possibly indicative of cell lysis and residual necromass left behind after fire (Donhauser et al., 2021) and compounded by the lightly combusted organic layer in the low severity soil. The relative contribution of aromatic and phenolic functional groups reached a maximum in the moderate severity soil extract, consistent with the calculated DBE and aromaticity index in the FT-ICR mass spectra (Table S5). These results are generally supported by previous studies across a wide range of environments, which reported increases in aromaticity following fire (Knicker et al., 2008). Our results also indicate that the changes observed in the DOM and SOM chemistry are unique from one another. It is likely that the changes in aromaticity observed in mineral soils are larger than those reported in the solution-state due to solubility limitations of the aromatic compounds. Therefore, both the mineral soil and water-soluble pools must be evaluated together to identify changes to C and N functionality that impact broader ecosystem functions.

# 3.3. Nitrogen composition of 0-5 cm soils was heavily influenced by fire activity

To further investigate the influence of fire on soil N species, we focused our analysis on the +ESI spectra, as this method has been reported to increase the compositional coverage of CHNO species compared to -ESI (Roth et al., 2022a). Table S4 reports the average O, C, N and C:N of each of the 0–5 cm soil samples determined by FT-ICR MS. We found that fire decreased the average C assigned for all burned soils compared to the unburned, though this value was not sensitive to burn severity. Average N per formula was  $3\times$  higher than the control for the low and moderate severity soils and was highest for the high severity soil. Increased N content has been reported in laboratory heating studies, attributed Maillard reactions and the formation of covalent bonds between ammonia and organic matter, but has not previously been reported from post-fire field studies (Bahureksa et al., 2022; Hestrin et al., 2019).

**Table 2** Integration results for solution-state  $^1$ H NMR spectroscopy for the 0–5 cm soil severity gradient (n = 1). Chemical shift is reported in parts per million (ppm). This table lists the relative proportion of each DOM category to the total signal of  $^1$ H across all regions.

	Relative proportion of soil-derived DOM categories to the total $^1\mathrm{H}$ NMR signal						
Sample	MDLT	CRAM	Carbohydrates &	Aromatic &			
	(0.6-1.6	(1.6-3.2)	peptides (3.2-4.5	phenolic			
	ppm)	ppm)	ppm)	(6.5-8.4 ppm)			
Control	34	37	22	7			
Low	38	31	27	4			
Moderate	34	32	25	9			
High	36	31	26	7			

Higher average N in burned soils greatly influenced the C:N ratio of the samples, which was lowest for the low severity soil. Enrichment of N species in burned soils has been observed in controlled lab settings (Bahureksa et al., 2022), and may be attributed to increases in pyridine, benzonitrile, and pyrrole functionalities at higher burn temperatures which were identified in soils affected by the 2013 Rim Fire in California (Chen et al., 2022c). Additionally, lysing of soil microorganisms during soil heating generates labile organic C and N that may contribute to increased dissolved N species following high severity wildfires (Donhauser et al., 2021).

Unique N species were compared across the burn severity gradient (Control vs Low, Low vs Moderate, and Moderate vs High) to determine the major changes which occur at each severity (Table 3). Because isotopes are not differentiated, there may be additional transformations that are not resolved here. From the control to low burn severity, 9817 unique N species were formed, likely from incomplete combustion of SOM (Bahureksa et al., 2022). Only 297 of the 5632 N species assigned in the control were unique, which indicates that the unique CHNO species in the low severity soil are likely newly formed. There was also a clear change in N speciation through the formation of molecules which are more N-dense (containing more N per molecule), which results in an expanded range of oxygenation and increased N in the low severity soil (Fig. S2A). From low to moderate severity, 3592 formulas were lost from the low severity soil, and 2153 species were newly formed in the moderate severity sample. Transformations occur across all N classes, and do not appear to preferentially impact any one class over another (Fig. S2B). From moderate to high severity, the largest losses were in the N<sub>1</sub> class (i.e., compound containing one N atom) and there were substantial increases in the N<sub>3</sub>-N<sub>5</sub> class (High) compared to the other transitions. The loss of N<sub>1</sub> formulas was primarily accompanied by a shift towards lower oxygen in the high severity soil from  $N_{1-3}$ , and a non-preferential increase in species containing  $N_{4-5}$  (Fig. S2C). N enrichment may be driven by several combustion-catalyzed processes, including the Maillard reaction pathway and the formation of covalent bonds between burned SOM and NH<sub>3</sub>-N (Bahureksa et al., 2022; Hestrin et al., 2019). These results suggest that soils that burned at higher severities contain higher polyaromatic N and are potentially more resistant to microbial degradation. Therefore, the observed decrease in C:N ratios in FT-ICR MS data may indicate a higher proportion of immobilized N, (e.g., as observed in char derived from lignin, cellulose, grass, and wood produced at 350 °C and 450 °C (Knicker, 2010)) rather than a highly preferential substrate as typically interpreted from C:N alone. Additionally, the N species identified may contribute to increased toxicity in water extracts (Bamba et al., 2017).

The m/z vs C:N of each CHNO species was plotted in Fig. 3 to visualize differences in molecular mass and N content along the burn severity gradient. We found that although the average mass of the formulas decreased as burn severity increased (Table S4), the relative abundance of nitrogenated high molecular weight species increased with burn severity. N-heterocyclic structures are known to form during incomplete combustion of SOM (Knicker et al., 2008), which is thought to be less

Table 3 Unique N species identified through + ESI FT-ICR MS of water-soluble soil extracts (0–5 cm). Unique formulas are determined only between the two samples compared, denoted in the top row.  $N_1$  includes molecules containing exactly one N,  $N_2$  includes molecules with two N atoms, etc.

Unique N species	Control vs Low		Low vs Moderate		Moderate vs High	
	Control	Low	Low	Moderate	Moderate	High
All N	297	9817	3592	2153	1499	1932
$N_1$	295	3464	2091	891	981	358
$N_2$	2	2850	670	560	346	410
$N_3$	N/A	1602	378	504	121	532
$N_4$	N/A	1338	261	126	39	379
N <sub>5</sub>	N/A	563	92	72	12	262

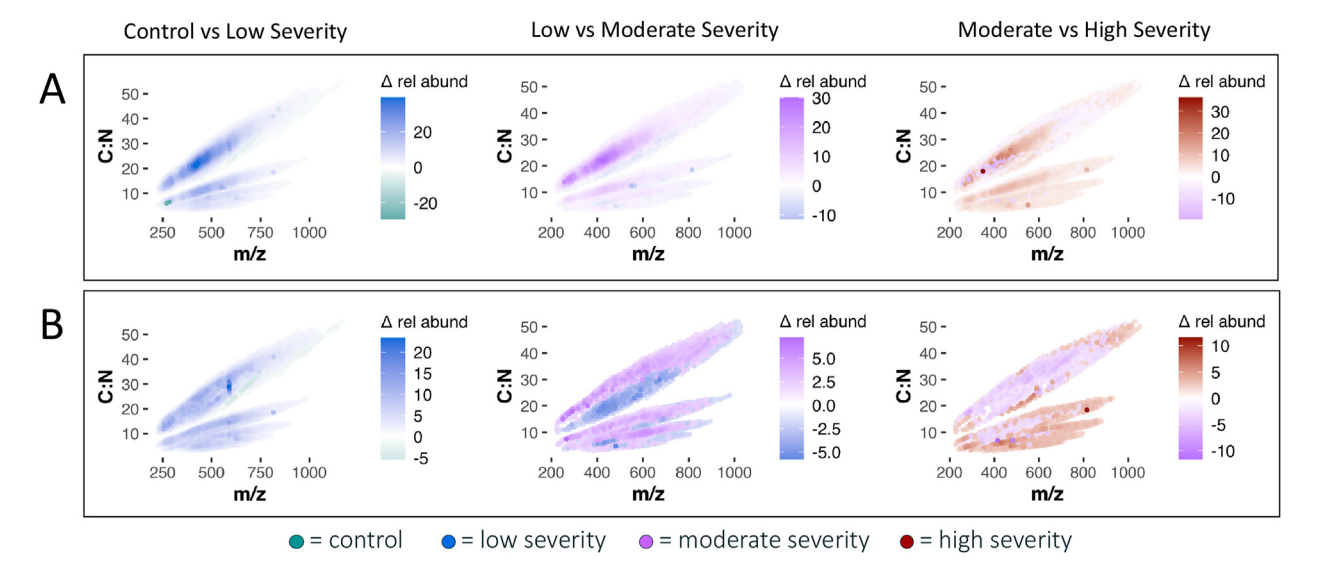


**Fig. 3.** Plots of the mass to charge (m/z) and nitrogen to carbon (N/C) ratios of the *N*-containing (i.e., CHNO) fraction obtained via + ESI FT-ICR MS of solid phase extracts of a single Ryan fire 0–5 cm soil burn severity gradient. Panel A displays plots with all the assigned N species; panel B displays only the unique species between the two spectra. Changes in relative abundance ( $\Delta$  rel abund) are indicated by darker colors. Green dots denote higher abundance in the control, and blue, purple, and red dots correspond to higher abundance in the low, moderate, and high severity extracts, respectively.

labile compared to unburned DON. The shift in DON functionality from peptides in unburned soils to polycyclic aromatic compounds (i.e., indoles and carbazoles) (Sharma et al., 2003) likely transforms SOM into a less bioavailable form, of which the microbial genes required for processing may not be widespread in the soil microbiome. To investigate this, we used HMMER (Eddy, 2011) against HMMs curated from UniProt (Bateman et al., 2015) to identify genes that constitute the primary enzyme for degrading carbazole (carbazole 1,9a-dioxgenase) (Nojiri et al., 2005) within the metagenome-assembled genome (MAG) dataset curated from these soils in Nelson et al. (2022). Of the total 637 MAGs, only 13 were actively expressing (via metatranscriptomics data) the majority of the genes required for the multicomponent enzymes (carAd, carAa, carAc), suggesting that these compounds are widely recalcitrant to bacterial degradation. Therefore, newly formed N species may represent an important N sink after fire in high severity burned lodgepole pine soils. Broad shifts in N speciation throughout the burn severity gradient, along with the loss of O-containing functional groups (Table S4), may be important for the previously reported differences in soil structure after burn and large alterations in microbial activity (Nelson et al., 2022).

## 3.4. The 0-5 cm soils are more influenced by fire than 5-10 cm soils

To determine how sampling depth influenced speciation, we compared the control and moderate soils at 0-5 cm and 5-10 cm sampling depths. The 5-10 cm control sample had 17,653 formulas assigned, 5032 of which contained N. Of the 17,870 formulas assigned to the 5-10 cm moderate soil, 6212 were N-containing. The increase in N species for the 5-10 cm soils is much smaller than the 0-5 cm soils, which increased from 5632 in the control to 13,813 in the moderate 0-5 cm soil. To further investigate the influence of fire on N species in 5-10 cm soils, we plotted the individual heteroatoms  $(N_xO_x)$  (Fig. S3). Between the 0–5 cm and 5–10 cm samples in the control, little variation is noted aside from the 0-5 cm soil being slightly shifted towards lower oxygenation compared to the 5-10 cm soil. There is a clear difference in N content, where the 0-5 cm samples are far more N-enriched than the 5-10 cm samples. These results are supported by previous literature indicating that fire generally impacts approximately the top 5 cm of mineral soils, with much less influence of heat further down the soil column (Hartford and Frandsen, 1992). However, we did note some important shifts between the control and moderate 5-10 cm soils, as illustrated in Fig. 4. Specifically, the moderate severity soil was shifted towards lower oxygen levels, consistent with our observations in the 0–5 cm samples. We also found that the more N-rich species ( $N_2$ – $N_4$ ) had far more assignments in the moderate severity soil compared to the control. Therefore, our results indicate that even though the largest effects are seen closer to the soil surface (i.e., 0–5 cm soils), the effects of fire on N speciation persist at least 10 cm down the soil column.

The relative contribution of all SOM categories determined by solidstate <sup>13</sup>C NMR was approximately the same for the 0-5 cm and 5-10 cm samples in the control soil (Table 1), consistent with the FT-ICR MS results and indicating that the organic horizon contributed minimally to the overall signal. However, there were notable differences between the 5-10 cm control and moderate severity soils. The relative proportion of O-alkyl C decreased by 10, while the aromatic and phenolic C signal increased by 11 in the moderate 5–10 cm soil compared to the control. Differences in the relative proportion of SOM signal indicate that the functional groups present in the soils were affected by the burn, even at the lower sampling depths. The moderate 0-5 cm soil was more aromatic and displayed a lower proportion of O-alkyl C than the 5-10 cm sample, consistent with previous studies reporting that the degree of carbonization and aromatization is lower in Pinus pinaster mineral soils than in duff (Merino et al., 2018). Because the 5-10 cm soil is not as highly impacted as the 0-5 cm soil, it likely contains more labile substrates for microbial degradation. The alkyl/O-alkyl C ratio supports this hypothesis, as the values are lower in the burned 5-10 cm soil than the 0-5 cm soil. Complementary metagenomics analyses indicated major shifts in microbial processing of substrates in 0-5 cm soils, which were not as prevalent in the 5-10 cm soils (Nelson et al., 2022). This suggests that while there are some differences in soil chemistry of the control and moderate 5-10 cm samples, these changes are not nearly as large as those in the 0-5 cm soils.

## 3.5. Acute toxicity of soil extract from fire-impacted soils as a function of burn severity

Carbon normalized water extracts of six soils were analyzed for acute toxicity by Microtox® to determine toxicity as a function of sample composition. Higher bioluminescence inhibition of *A. fischeri* corresponds to higher acute toxicity. We observed an increase in toxicity with increasing burn severity in the 0–5 cm soils (Fig. 5), and no change in the 5–10 cm soils. Among the 0–5 cm soils, the high severity 0–5 cm soil had the highest acute toxicity (43%) followed by moderate severity 0–5 cm soil (17%) and low severity 0–5 cm soil (10%).

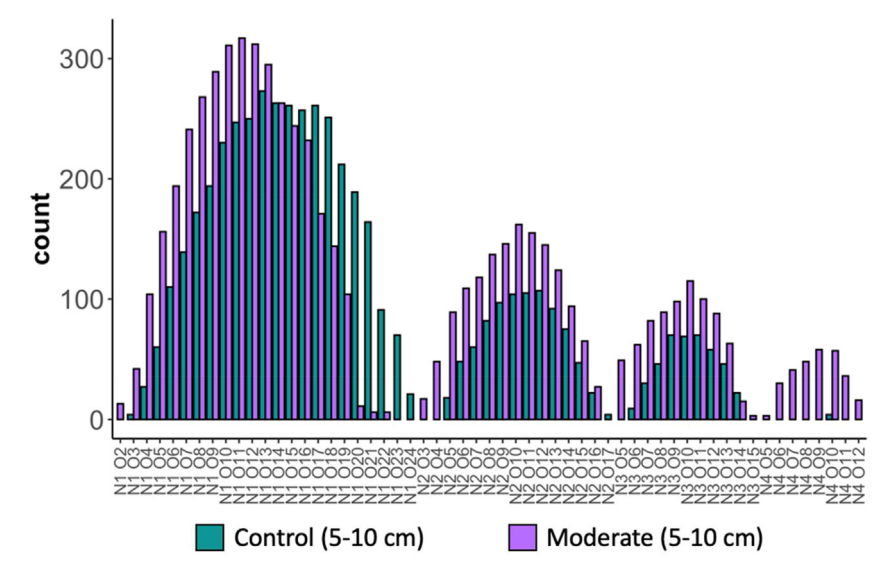


Fig. 4. Nitrogen-containing classes in control and moderate severity 5–10 cm samples (n = 1) from +ESI FT-ICR MS. The x-axis is organized by heteroatoms, grouped first by the number of N atoms (1–4) assigned to the formulas and second by the number of oxygen atoms. The y-axis depicts the number of formulas assigned to each heteroatom class.

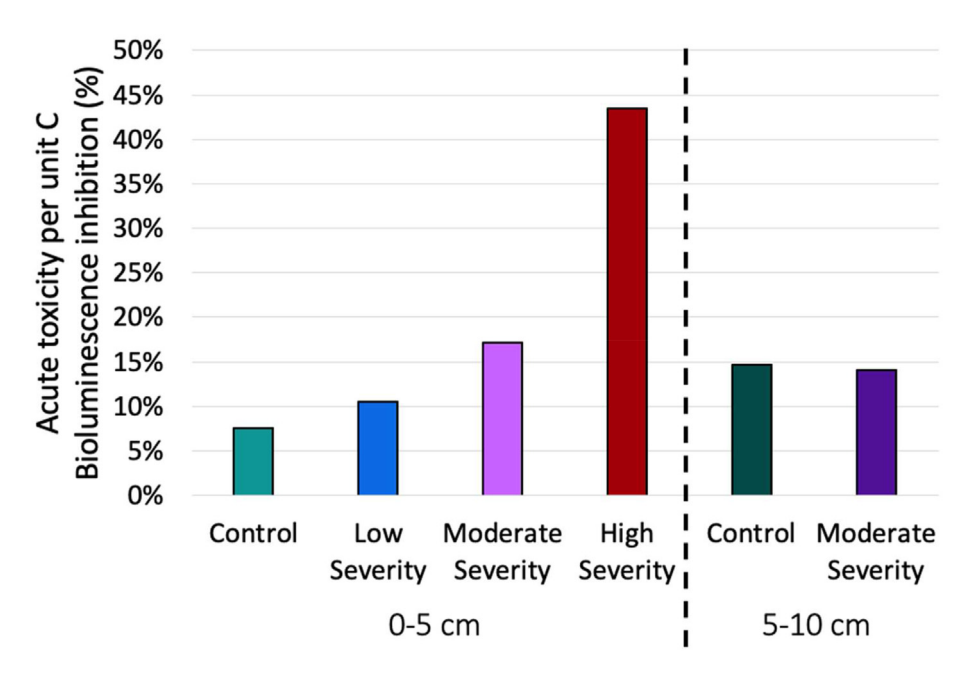


Fig. 5. The 15 min % bioluminescence inhibition of burned soil water extracts (n = 1); higher % inhibition corresponds to higher toxicity.

Microtox® bioassays have previously been applied to determine the acute toxicity of aqueous ash extracts and runoff following wildfires, both of which inhibited the luminescence of A. fischeri (Campos et al., 2012; Silva et al., 2015). Toxicity increases with ash concentration (Silva et al., 2015), and more "complete" combustion in high severity soils may explain the increase in toxicity reported here. A toxicity study using Daphnia magna found pH to be a strong influence on toxicity (Harper et al., 2019); however, pH cannot explain the increases in toxicity seen here, as maximum pH values were observed in the moderate severity 0-5 cm soil (average pH = 8.00), whereas the 5-10 cm samples did not appear to be affected (average pH ranging between 7.11 and 7.71) (Table S4). Previous studies indicated that the formation of *N*-heterocycles may contribute to increased toxicity (Cervilla et al., 2009), which likely contributes to the observed increase in toxicity here. However, further research is required to identify the specific drivers of toxicity increases in burned organic matter, such as polycyclic aromatic

hydrocarbons or heavy metals released during burning. The observed toxicity increase in 0–5 cm soil extracts emphasizes the role of wildfire as a potential source of diffuse contamination for downstream water bodies.

## 4. Conclusions

Molecular-level analysis of C and N contained in soil organic matter across a burn severity gradient allowed us to make inferences regarding how organic N is altered by wildfire in high-elevation forests. Although high-resolution results for a single gradient are reported here, trends identified from bulk data collected from four burn severity gradients indicate that these results are likely representative of all the soils we collected. While the analysis of a single gradient does not allow for statistical analysis, advanced analytical approaches involve rigorous internal calibration that ensures the resulting data are accurate. Therefore, the molecular-level information provided by our unique integrative

analytical approach provides novel evidence for a potential relationship between chemistry, toxicity, and the soil microbiome. Our results suggest that *N*-dense heterocycles (e.g., carbazoles, indoles) are formed at higher fire severities, which has implications for post-fire C and N cycling since evidence for processing of these compounds was not widespread in the local soil microbiome. We noted a shift in N speciation for the 5–10 cm soil depth, which indicates that heating at that depth was sufficient to shift SOM chemistry. We also provide evidence that soil toxicity is dependent on burn severity, although further research is required to identify the specific drivers of soil toxicity and the potential downstream effects. Collectively, these results emphasize the importance of molecular-level characterization of SOM components to evaluate the impacts of fire on C and N biogeochemistry and provide new insight into the impact of severe wildfire on forest ecosystems.

## **Declaration of Competing Interest**

The authors have no potential competing interests.

#### Acknowledgements

DOC and DTN measurements were conducted at the Rocky Mountain Research Station, biogeochemistry laboratory, courtesy of the USDA Forest Service. The authors acknowledge support of MJW and TB from the National Science Foundation under grant number 2114868 and USDA National Institute of Food and Agriculture through AFRI grant number 2021-67019-34608. A portion of the work was performed at the National High Magnetic Field Laboratory ICR User Facility, which is supported by the National Science Foundation Division of Chemistry and Division of Material Research through DMR-1644779 and the State of Florida. M.J.S. thanks the Natural Sciences and Engineering Research Council (NSERC) of Canada for support via a Discovery Grant and the Tier 1 Canada Research Chair in Integrative Molecular Biogeochemistry.

## Appendix A. Supplementary data

Supplementary data to this article can be found online at https://doi. org/10.1016/j.seh.2023.100023.

### References

- Abatzoglou, J.T., Kolden, C.A., Williams, A.P., Lutz, J.A., Smith, A.M.S., 2017. Climatic influences on interannual variability in regional burn severity across western US forests. Int. J. Wildland Fire 26, 269–275. https://doi.org/10.1071/WF16165.
- Adams, R.H., Domínguez-Rodríguez, V.I., Zavala-Cruz, J., 2015. Vibrio fischeri bioassay for determination of toxicity in petroleum contaminated soils from tropical southeast Mexico. Sains Malays. 44, 337–346.
- Alimoradi, S., Stohr, H., Stagg-Williams, S., Sturm, B., 2020. Effect of temperature on toxicity and biodegradability of dissolved organic nitrogen formed during hydrothermal liquefaction of biomass. Chemosphere 238. https://doi.org/10.1016/ j.chemosphere.2019.124573.
- Alizadeh, M.R., Abatzoglou, J.T., Luce, C.H., Adamowski, J.F., Farid, A., Sadegh, M., 2021. Warming enabled upslope advance in western US forest fires. Proc. Natl. Acad. Sci. USA 118. https://doi.org/10.1073/pnas.2009717118/-/DCSupplemental.
- Andersson, S., Nilsson, S.I., Saetre, P., 2000. Leaching of dissolved organic carbon (DOC) and dissolved organic nitrogen (DON) in mor humus as affected by temperature and pH. Soil Biol. Biogeochem. 32, 1–10.
- Bahureksa, W., Young, R.B., McKenna, A.M., Chen, H., Thorn, K.A., Rosario-Ortiz, F.L., Borch, T., 2022. Nitrogen enrichment during soil organic matter burning and molecular evidence of maillard reactions. Environ. Sci. Technol. https://doi.org/ 10.1021/acs.est.1c06745.
- Bamba, D., Coulibaly, M., Robert, D., 2017. Nitrogen-containing Organic Compounds: Origins, Toxicity and Conditions of Their Photocatalytic Mineralization over TiO2. Science of the Total Environment. https://doi.org/10.1016/j.scitotenv.2016.12.130.
- Bateman, A., Martin, M.J., O'Donovan, C., Magrane, M., Apweiler, R., Alpi, E., Antunes, R., Arganiska, J., Bely, B., Bingley, M., Bonilla, C., Britto, R., Bursteinas, B., Chavali, G., Cibrian-Uhalte, E., da Silva, A., de Giorgi, M., Dogan, T., Fazzini, F., Gane, P., Castro, L.G., Garmiri, P., Hatton-Ellis, E., Hieta, R., Huntley, R., Legge, D., Liu, W., Luo, J., Macdougall, A., Mutowo, P., Nightingale, A., Orchard, S., Pichler, K., Poggioli, D., Pundir, S., Pureza, L., Qi, G., Rosanoff, S., Saidi, R., Sawford, T., Shypitsyna, A., Turner, E., Volynkin, V., Wardell, T., Watkins, X., Zellner, H., Cowley, A., Figueira, L., Li, W., McWilliam, H., Lopez, R., Xenarios, I., Bougueleret, L., Bridge, A., Poux, S., Redaschi, N., Aimo, L., Argoud-Puy, G., Auchincloss, A.,

- Axelsen, K., Bansal, P., Baratin, D., Blatter, M.C., Boeckmann, B., Bolleman, J., Boutet, E., Breuza, L., Casal-Casas, C., de Castro, E., Coudert, E., Cuche, B., Doche, M., Dornevil, D., Duvaud, S., Estreicher, A., Famiglietti, L., Feuermann, M., Gasteiger, E., Gehant, S., Gerritsen, V., Gos, A., Gruaz-Gumowski, N., Hinz, U., Hulo, C., Jungo, F., Keller, G., Lara, V., Lemercier, P., Lieberherr, D., Lombardot, T., Martin, X., Masson, P., Morgat, A., Neto, T., Nouspikel, N., Paesano, S., Pedruzzi, I., Pilbout, S., Pozzato, M., Pruess, M., Rivoire, C., Roechert, B., Schneider, M., Sigrist, C., Sonesson, K., Staehli, S., Stutz, A., Sundaram, S., Tognolli, M., Verbregue, L., Veuthey, A.L., Wu, C.H., Arighi, C.N., Arminski, L., Chen, C., Chen, Y., Garavelli, J.S., Huang, H., Laiho, K., McGarvey, P., Natale, D.A., Suzek, B.E., Vinayaka, C.R., Wang, Q., Wang, Y., Yeh, L.S., Yerramalla, M.S., Zhang, J., 2015. UniProt: a hub for protein information. Nucleic Acids Res. 43, D204–D212. https://doi.org/10.1093/nar/eku989
- Belov, M.E., Rakov, V.S., Nikolaev, E.N., Goshe, M.B., Anderson, G.A., Smith, R.D., 2003. Initial implementation of external accumulation liquid chromatography/electrospray ionization fourier transform ion cyclotron resonance with automated gain control. Rapid Commun. Mass Spectrom. 17, 627–636. https://doi.org/10.1002/rcm.955.
- Bodí, M.B., Martin, D.A., Balfour, V.N., Santín, C., Doerr, S.H., Pereira, P., Cerdà, A., Mataix-Solera, J., 2014. Wildland fire ash: production, composition and eco-hydro-geomorphic effects. Earth Sci. Rev. 130, 103–127. https://doi.org/10.1016/j.earscirev.2013.12.007.
- Caiafa, M.V., Nelson, A.R., Borch, T., Roth, H.K., Fegel, T.S., Rhoades, C.C., Wilkins, M.J., Glassman, S.I., 2023. Distinct fungal and bacterial responses to fire severity and soil depth across a ten-year wildfire chronosequence in beetle-killed lodgepole pine forests. For. Ecol. Manag. 544, 121160. https://doi.org/10.1016/ j.foreco.2023.121160.
- Campos, I., Abrantes, N., Vidal, T., Bastos, A.C., Gonçalves, F., Keizer, J.J., 2012.
  Assessment of the toxicity of ash-loaded runoff from a recently burnt eucalypt plantation. Eur. J. For. Res. 131, 1889–1903. https://doi.org/10.1007/s10342-012-0640-7
- Cervilla, L.M., Blasco, B., Ríos, J.J., Rosales, M.A., Rubio-Wilhelmi, M.M., Sánchez-Rodríguez, E., Romero, L., Ruiz, J.M., 2009. Response of nitrogen metabolism to boron toxicity in tomato plants. Plant Biol. 11, 671–677. https://doi.org/10.1111/j.1438-8677.2008.00167.x.
- Chen, H., Ersan, M.S., Tolić, N., Chu, R.K., Karanfil, T., Chow, A.T., 2022a. Chemical characterization of dissolved organic matter as disinfection byproduct precursors by UV/fluorescence and ESI FT-ICR MS after smoldering combustion of leaf needles and woody trunks of pine (Pinus jeffreyi). Water Res. 209. https://doi.org/10.1016/ j.watres.2021.117962.
- Chen, H., McKenna, A.M., Niles, S.F., Frye, J.W., Glattke, T.J., Rodgers, R.P., 2022b. Time-dependent molecular progression and acute toxicity of oil-soluble, interfacially-active, and water-soluble species reveals their rapid formation in the photodegradation of Macondo Well Oil. Sci. Total Environ. 813. https://doi.org/10.1016/j.scijotenv.2021.151884.
- Chen, H., Wang, J.-J., Ku, P.-J., Tsui, M.T.-K., Abney, R.B., Berhe, A.A., Zhang, Q., Burton, S.D., Dahlgren, R.A., Chow, A.T., 2022c. Burn intensity drives the alteration of phenolic lignin to (Poly) aromatic hydrocarbons as revealed by pyrolysis gas chromatography–mass spectrometry (Py-GC/MS). Environ. Sci. Technol. https:// doi.org/10.1021/acs.est.2c00426.
- Corilo, Y.E., 2014. PetroOrg Software.
- D'Andrilli, J., Cooper, W.T., Foreman, C.M., Marshall, A.G., 2015. An ultrahigh-resolution mass spectrometry index to estimate natural organic matter lability. Rapid Commun. Mass Spectrom. 29, 2385–2401. https://doi.org/10.1002/rcm.7400.
- Dittmar, T., Koch, B., Hertkorn, N., Kattner, G., 2008. A simple and efficient method for the solid-phase extraction of dissolved organic matter (SPE-DOM) from seawater. Limnol Oceanogr. Methods 6, 230–235.
- Doherty, F.G., 2001. A Review of the Microtox ® toxicity test system for assessing the toxicity of sediments and soils. Water Qual. Res. J. Can. 36, 475–518.
- Donhauser, J., Qi, W., Bergk-Pinto, B., Frey, B., 2021. High temperatures enhance the microbial genetic potential to recycle C and N from necromass in high-mountain soils. Global Change Biol. 27, 1365–1386. https://doi.org/10.1111/gcb.15492.
- Dzwonko, Z., Loster, S., Gawroński, S., 2015. Impact of fire severity on soil properties and the development of tree and shrub species in a Scots pine moist forest site in southern Poland. Ecol. Manag. 342, 56–63. https://doi.org/10.1016/j.foreco.2015.01.013.
- Eddy, S.R., 2011. Accelerated profile HMM searches. PLoS Comput. Biol. 7. https://doi.org/10.1371/journal.pcbi.1002195.
- Emmett, M.R., White, F.M., Hendrickson, C.L., Shi, D.H., Marshall, A.G., 1998.
  Application of micro-electrospray liquid chromatography techniques to FT-ICR MS to enable high-sensitivity biological analysis. J. Am. Soc. Mass Spectrom. 9, 333–340. https://doi.org/10.1016/S1044-0305(97)00287-0.
- González-Pérez, J.A., González-Vila, F.J., Almendros, G., Knicker, H., 2004. The effect of fire on soil organic matter - a review. Environ. Int. 30, 855–870. https://doi.org/ 10.1016/j.envint.2004.02.003.
- Harper, A.R., Santin, C., Doerr, S.H., Froyd, C.A., Albini, D., Otero, X.L., Viñas, L., Pérez-Fernández, B., 2019. Chemical composition of wildfire ash produced in contrasting ecosystems and its toxicity to Daphnia magna. Int. J. Wildland Fire 28, 726–737. https://doi.org/10.1071/WF18200.
- Hartford, R.A., Frandsen, W.H., 1992. When it's hot, it's hot ... or maybe it's not! (Surface flaming may not portend extensive soil heating). Int. J. Wildland Fire 2 (3), 139–144.
- Hendrickson, C.L., Quinn, J.P., Kaiser, N.K., Smith, D.F., Blakney, G.T., Chen, T., Marshall, A.G., Weisbrod, C.R., Beu, S.C., 2015. 21 Tesla fourier transform ion cyclotron resonance mass spectrometer: a national resource for ultrahigh resolution

- mass analysis. J. Am. Soc. Mass Spectrom. 26, 1626–1632. https://doi.org/10.1007/s13361-015-1182-2.
- Hestrin, R., Torres-Rojas, D., Dynes, J.J., Hook, J.M., Regier, T.Z., Gillespie, A.W., Smernik, R.J., Lehmann, J., 2019. Fire-derived organic matter retains ammonia through covalent bond formation. Nat. Commun. 10, 1–8. https://doi.org/10.1038/ s41467-019-08401-z.
- Key, C.H., Benson, N.C., 2006. Landscape Assessment (LA) Sampling and Analysis Methods. USDA Forest Service Gen Tech. Rep RMRS-GTR-164-CD.
- Kim, S., Kramer, R.W., Hatcher, P.G., 2003. Graphical method for analysis of ultrahighresolution broadband mass spectra of natural organic matter, the Van Krevelen diagram. Anal. Chem. 75, 5336–5344. https://doi.org/10.1021/ac034415p.
- Knicker, H., 2010. "Black nitrogen" an important fraction in determining the recalcitrance of charcoal. Org. Geochem. 41, 947–950. https://doi.org/10.1016/ i.orgeochem.2010.04.007.
- Knicker, H., Hilscher, A., González-Vila, F.J., Almendros, G., 2008. A new conceptual model for the structural properties of char produced during vegetation fires. Org. Geochem. 39, 935–939. https://doi.org/10.1016/j.orggeochem.2008.03.021.
- Luo, L., Chen, Z., Lv, J., Cheng, Y., Wu, T., Huang, R., 2019. Molecular understanding of dissolved black carbon sorption in soil-water environment. Water Res. 154, 210–216. https://doi.org/10.1016/j.watres.2019.01.060.
- Merino, A., Chávez-Vergara, B., Salgado, J., Fonturbel, M.T., García-Oliva, F., Vega, J.A., 2015. Variability in the composition of charred litter generated by wildfire in different ecosystems. Catena 133, 52–63. https://doi.org/10.1016/ j.catena.2015.04.016.
- Merino, A., Fonturbel, M.T., Fernández, C., Chávez-Vergara, B., García-Oliva, F., Vega, J.A., 2018. Inferring changes in soil organic matter in post-wildfire soil burn severity levels in a temperate climate. Sci. Total Environ. 627, 622–632. https:// doi.org/10.1016/j.scitotenv.2018.01.189.
- Moody, J.A., Shakesby, R.A., Robichaud, P.R., Cannon, S.H., Martin, D.A., 2013. Current research issues related to post-wildfire runoff and erosion processes. Earth Sci. Rev. 122, 10–37. https://doi.org/10.1016/j.earscirev.2013.03.004.
- Nave, L.E., Vance, E.D., Swanston, C.W., Curtis, P.S., 2011. Fire effects on temperate forest soil C and N storage. Ecol. Appl. 21, 1189–1201. https://doi.org/10.1890/10-0660.1.
- Nelson, A.R., Narrowe, A.B., Rhoades, C.C., Fegel, T.S., Daly, R.A., Roth, H.K., Chu, R.K., Amundson, K.K., Young, R.B., Steindorff, A.S., Mondo, S.J., Grigoriev, I.V., Salamov, A., Borch, T., Wilkins, M.J., 2022. Wildfire-dependent changes in soil microbiome diversity and function. Nat Microbiol. https://doi.org/10.1038/s41564-022-01203-v.
- Nojiri, H., Ashikawa, Y., Noguchi, H., Nam, J.W., Urata, M., Fujimoto, Z., Uchimura, H., Terada, T., Nakamura, S., Shimizu, K., Yoshida, T., Habe, H., Omori, T., 2005. Structure of the terminal oxygenase component of angular dioxygenase, carbazole 1,9a-dioxygenase. J. Mol. Biol. 351, 355–370. https://doi.org/10.1016/i.imb.2005.05.059.
- Page, J.S., Bogdanov, B., Vilkov, A.N., Prior, D.C., Buschbach, M.A., Tang, K., Smith, R.D., 2005. Automatic gain control in mass spectrometry using a jet disrupter electrode in an electrodynamic ion funnel. J. Am. Soc. Mass Spectrom. 16, 244–253. https:// doi.org/10.1016/j.jasms.2004.11.003.
- Parsons, A., Robichaud, P.R., Lewis, S.A., Napper, C., Clark, J.T., 2010. Field Guide for Mapping Post-Fire Soil Burn Severity. General Technical Report RMRS-GTR-243.
- Pulido-Chavez, M.F., Alvarado, E.C., DeLuca, T.H., Edmonds, R.L., Glassman, S.I., 2021. High-severity wildfire reduces richness and alters composition of ectomycorrhizal fungi in low-severity adapted ponderosa pine forests. Ecol. Manag. 485. https:// doi.org/10.1016/j.foreco.2021.118923.

- Rhoades, C.C., Chow, A.T., Covino, T.P., Fegel, T.S., Pierson, D.N., Rhea, A.E., 2018. The legacy of a severe wildfire on stream nitrogen and carbon in headwater catchments. Ecosystems. https://doi.org/10.1007/s10021-018-0293-6.
- Roth, H.K., Borch, T., Young, R.B., Bahureksa, W., Blakney, G.T., Nelson, A.R., Wilkins, M.J., McKenna, A.M., 2022a. Enhanced speciation of pyrogenic organic matter from wildfires enabled by 21 T FT-ICR mass spectrometry. Anal Chem. https://doi.org/10.1021/acs.analchem.1c05018.
- Roth, H.K., Nelson, A.R., McKenna, A.M., Fegel, T.S., Young, R.B., Rhoades, C.C., Wilkins, M.J., Borch, T., 2022b. Impact of beaver ponds on biogeochemistry of organic carbon and nitrogen along a fire-impacted stream. Environ Sci Process Impacts 24, 1661–1677. https://doi.org/10.1039/D2EM00184E.
- Schmidt, M.W.I., Noack, A.G., 2000. Black carbon in soils and sediments: analysis, distribution, implications, and current challenges. Global Biogeochem Cycles. https://doi.org/10.1029/1999GB001208.
- Schmidt, M.W.I., Torn, M.S., Abiven, S., Dittmar, T., Guggenberger, G., Janssens, I.A., Kleber, M., Kögel-Knabner, I., Lehmann, J., Manning, D.A.C., Nannipieri, P., Rasse, D.P., Weiner, S., Trumbore, S.E., 2011. Persistence of soil organic matter as an ecosystem property. Nature 478, 49–56. https://doi.org/10.1038/nature10386.
- Sharma, R.K., Chan, W.G., Seeman, J.I., Hajaligol, M.R., 2003. Formation of low molecular weight heterocycles and polycyclic aromatic compounds (PACs) in the pyrolysis of a-amino acids. J. Anal. Appl. Pyrolysis 66, 97–121.
- Silva, V., Pereira, J.L., Campos, I., Keizer, J.J., Gonçalves, F., Abrantes, N., 2015. Toxicity assessment of aqueous extracts of ash from forest fires. Catena 135, 401–408. https:// doi.org/10.1016/j.catena.2014.06.021.
- Simpson, M.J., Otto, A., Feng, X., 2008. Comparison of Solid-State Carbon-13 Nuclear magnetic resonance and organic matter biomarkers for assessing soil organic matter degradation. Soil Sci. Soc. Am. J. 72, 268–276. https://doi.org/10.2136/ sssai2007.0045.
- Singh, N., Abiven, S., Torn, M.S., Schmidt, M.W.I., 2012. Fire-derived organic carbon in soil turns over on a centennial scale. Biogeosciences 9, 2847–2857. https://doi.org/ 10.5194/bg-9-2847-2012.
- Smith, D.F., Podgorski, D.C., Rodgers, R.P., Blakney, G.T., Hendrickson, C.L., 2018. 21 Tesla FT-ICR mass spectrometer for ultrahigh-resolution analysis of complex organic mixtures. Anal. Chem. 90, 2041–2047. https://doi.org/10.1021/ acs.analchem.7b04159.
- Smolander, Aino, Kitunen, Veikko, Mälkönen, Eino, Smolander, A., Kitunen, V., Mälkönen, E., 2001. Dissolved soil organic nitrogen and carbon in a Norway spruce stand and an adjacent clear-cut. Biol Fertil Soils.
- Turner, M.G., 2010. Disturbance and Landscape Dynamics in a Changing World 91, pp. 2833–2849.
- Wan, S., Hui, D., Luo, Y., 2001. Fire effects on nitrogen pools and dynamics in terrestrial ecosystems: a meta-analysis. Ecol. Appl.
- Westerling, A.L.R., 2016. Increasing western US forest wildfire activity: sensitivity to changes in the timing of spring. Phil. Trans. Biol. Sci. 371. https://doi.org/10.1098/ rstb.2015.0178.
- Williams, A.P., Abatzoglou, J.T., 2016. Recent advances and remaining uncertainties in resolving past and future climate effects on global fire activity. Curr. Clim. Change Rep. https://doi.org/10.1007/s40641-016-0031-0.
- Xu, P., Yu, B., Li, F.L., Cai, X.F., Ma, C.Q., 2006. Microbial degradation of sulfur, nitrogen and oxygen heterocycles. Trends Microbiol. https://doi.org/10.1016/ i.tim.2006.07.002.
- Zhong, Z., Makeschin, F., 2003. Soluble organic nitrogen in temperate forest soils. Soil Biol. Biogeochem. 35, 333–338.